

## Mutant Met121Ala of *Pseudomonas aeruginosa* Azurin and Its Azide Derivative: Crystal Structures and Spectral Properties

LI-CHU TSAI,<sup>a</sup> NICKLAS BONANDER,<sup>b</sup> KAZUAKI HARATA,<sup>c</sup> GÖRAN KARLSSON,<sup>b</sup> TORE VÄNNGÅRD,<sup>b</sup> VRATISLAV LANGER<sup>a</sup> AND LENNART SJÖLIN<sup>a</sup>

<sup>a</sup>Department of Inorganic Chemistry, Chalmers University of Technology and Göteborg University, S-412 96 Göteborg, Sweden, <sup>b</sup>Department of Biochemistry and Biophysics, Lundberg Laboratory, Chalmers University of Technology and Göteborg University, S-413 90 Göteborg, Sweden, and <sup>c</sup>Department of Biomolecules, National Institute of Bioscience and Human-Technology, 1-1 Higashi, Tsukuba, Ibaraki 305, Japan

(Received 27 September 1995; accepted 16 April 1996)

### Abstract

The crystal structures of the azurin mutant Met121Ala and its azide derivative Met121Ala-azide from *Pseudomonas aeruginosa* have been determined. The final crystallographic *R* values are 21.3 and 19.4% for the two structures, respectively. In the Met121Ala mutant, the distance between the copper ion and His117 increases by 0.34 Å compared with the wild-type structure. The removal of the methionine in the apical position induces a shortening of the distance from the copper ion to the carbonyl O atom of Gly45 from 2.97 to 2.74 Å. In the Met121Ala-azide structure, the azide anion occupies the cavity created by replacing the Met121 side chain with the smaller methyl group of Ala. The azide anion binds with a terminal N atom to the copper ion at a distance of about 2.04 Å. In addition, the copper ion has moved out of the trigonal plane by about 0.26 Å towards the azide anion. Thus, the copper site in this structure has a distorted tetrahedral arrangement. The spectroscopic characteristics show, in addition, that the copper sites in the two structures are distinctively different. The Met121Ala mutant still maintains the properties of an ordinary type 1 copper site while the Met121Ala-azide derivative has an absorption maximum at about 409 nm and the copper hyperfine coupling has increased to a value intermediate between those of type 2 copper and the wild-type azurin.

### 1. Introduction

In the past 25 years, type 1 blue-copper proteins have attracted many investigators because of their unusual physical and chemical properties. The most significant properties of these proteins are the blue color resulting from an intense optical absorption at about 600 nm and a unique hyperfine splitting in the electron paramagnetic resonance (EPR) spectra. Many studies have been focused on defining the copper center and the relationships between its structure and spectroscopic properties.

The type 1 copper site is generally involved in mediating electron transfer, and the type 1 proteins exhibit

relatively high midpoint potentials (Reinhammar, 1972). From the structural work carried out in the late 1970's on azurin and plastocyanin (Adman, Stenkamp, Sieker & Jensen, 1978; Colman *et al.*, 1978) and later crystal structure determinations on type 1 blue proteins (for a review see Adman, 1991), the copper site has been unambiguously determined. The copper ion is coordinated by three strong ligands, two histidine residues and a cysteine residue. A fourth weaker interaction to a methionine in the apical position has also been discussed. The distance between the copper and the S atom of the axial methionine is in the range of 2.62 Å (cucumber basic blue protein) to 3.25 Å (azurin). In addition a fifth potential ligand, a carbonyl O atom, is found in azurin, algal plastocyanin and amicyanin. The distance between the copper and the carbonyl O atom is in the range 2.75–3.22 Å (Adman, 1991; Dodd, Hasnain, Abraham, Eady & Smith, 1995).

The three strong copper ligands in the azurin molecule have previously been mutated and the mutants have been studied using spectroscopic methods. Chang *et al.* (1991) investigated the effects of a replacement of His46 for Asp46 and found that the Asp46 side chain binds to the copper ion in the metal site with a geometry similar to that in the wild-type azurin structure. Consequently, the EPR and optical spectra were almost unchanged. However, when Cys112 was replaced by Asp112 it was found that the ligand bond to the copper ion was maintained but the spectroscopic measurements indicated that the copper site no longer was of type 1 but of type 2 (Mizoguchi, Bilio, Gray & Richards, 1992). When the third ligand, His117, was mutated to Gly117, several different small molecules could enter the pocket that was created, and, depending on the nature of this molecule, both type 1 and type 2 sites were obtained (den Blaauwen, van de Kamp & Canters, 1991; den Blaauwen & Canters, 1993).

The methionine ligand has been suggested as an important amino-acid residue for tuning the redox potential (Gray & Malmström, 1983). This was supported by the fact that stellacyanin, the only type 1 blue protein known

to lack a methionine in the apical direction at that time, has the lowest reduction potential (184 mV) of the blue-copper proteins (Fields, Guss & Freeman, 1991). The importance of methionine for tuning the redox potential has later been confirmed in a cassette mutagenesis study conducted on this residue in azurin from *Pseudomonas aeruginosa* (Karlsson *et al.*, 1991). The Met121 residue was mutated into all the other 19 amino-acid residues and the reduction potential of 13 of these mutants was measured. The reduction potentials were found to be in

the range 180–450 mV, and it was concluded that a low reduction potential is obtained if a negatively charged or hydrophilic residue replaces the methionine. Conversely, an azurin with a high reduction potential is constructed

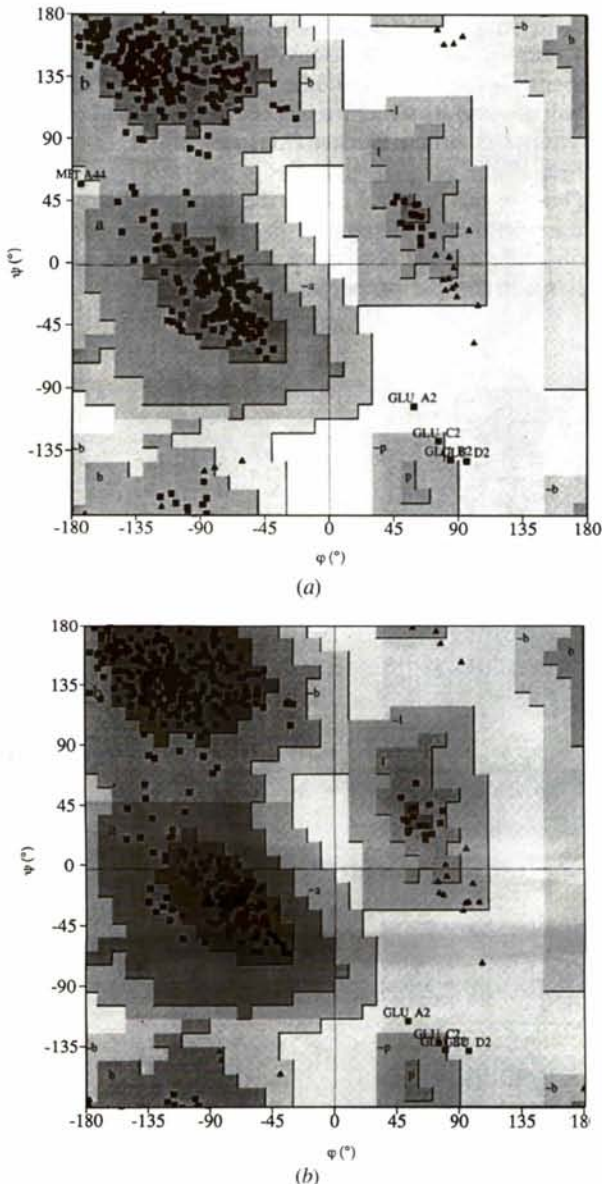


Fig. 1. Ramachandran plot of main-chain dihedral angles for (a) the Met121Ala tetramer and (b) the Met121Ala-azide tetramer (molecules, A, B, C and D). The plot was calculated using PROCHECK (Laskowski, MacArthur, Moss & Thornton, 1993). Glycine residues are shown as triangles and the other residues as squares. Residues Glu2A, 2B, 2C, 2D in (a) and (b), and Met44 in (b) with conformational angles outside allowed regions are labeled.

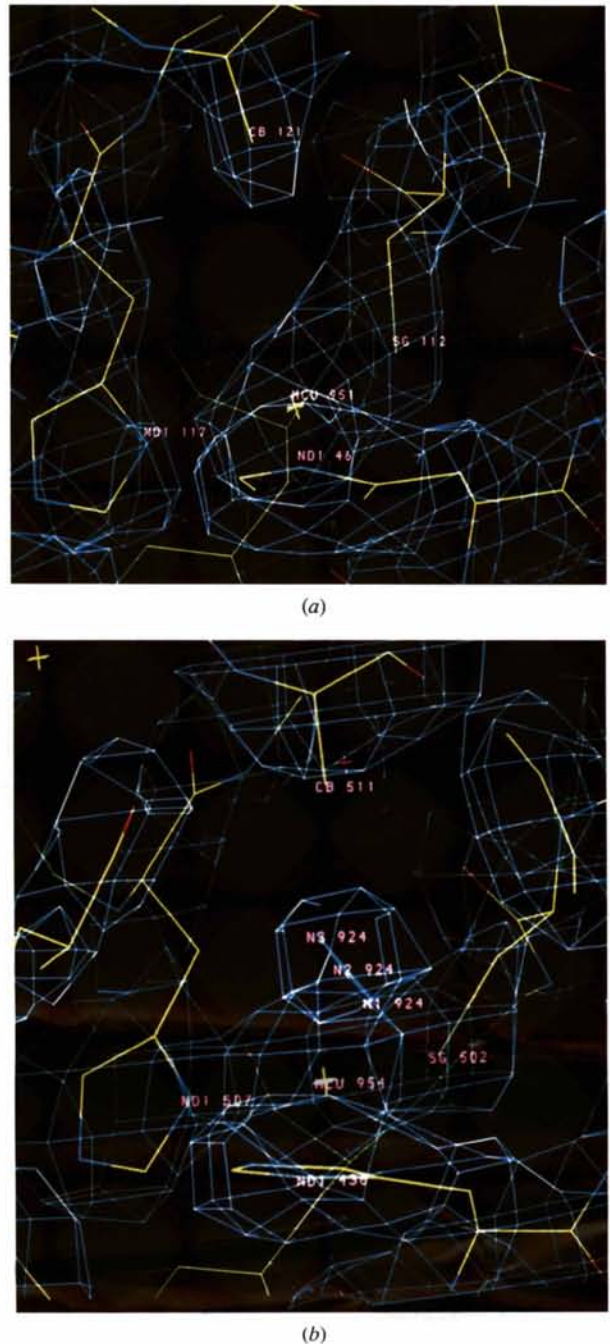


Fig. 2. (a) The mutation site in the Met121Ala mutant structure and (b) the mutation site with azide anion in the Met121Ala-azide mutant structure (molecule D). The labels ND1 436, SG 502, ND1 507, and CB 511 refer to atoms  $N^{\delta 1}$  46,  $S^{\gamma 1}$  112,  $N^{\delta 1}$  117, and  $C^{\beta}$  121 in molecule D, respectively. The  $2F_o - F_c$  electron-density maps contoured at  $1.0\sigma$ .

when a hydrophobic amino-acid residue like leucine or valine replaces the methionine.

Two mutant structures in position 121, Glu121 and Leu121, representing the two different categories (low and high reduction potential) have previously been determined by X-ray analysis to investigate the structural differences in the metal site (Karlsson *et al.*, 1996). Moreover, the X-ray analysis and complementary spectroscopic characterization of the related stellacyanin-like Met121Gln mutant have been conducted by Romero *et al.* (1993).

When the Met121 is exchanged for alanine, which represents a small hydrophobic residue, a free space may be created between this amino acid and the copper site. Spectroscopic investigations of this mutant have not, however, indicated that any water molecule has been trapped in this free space. By adding small anionic molecules to the protein solution it was eventually found by spectroscopic measurements that molecules such as azide, cyanide and acetate could diffuse into the metal site to become an exogenous ligand to the

copper ion (Bonander, Karlsson & Vänngård, 1996) and thereby another possible way to tune the redox potential has emerged. The spectroscopic data obtained from the azide-modified azurin Met121Ala mutant show that the copper site is different from the normal type 1 copper site.

To study in detail the similarities and differences between the wild-type azurin metal site and the Met121Ala mutant with and without an additional azide anionic molecule we have solved the latter two mutant structures using X-ray diffraction methods. The diffusion of an azide molecule into a protein metal site has been reported in a number of investigations. However, the modified copper site has been studied by X-ray diffraction techniques and its structure has been determined only in the case of ascorbate oxidase (Messerschmidt, Luecke & Huber, 1993).

Thus, in this report we describe the crystal structures of the Met121Ala mutant of *Pseudomonas aeruginosa* azurin and its azide derivative. We also present some of their spectroscopic properties.

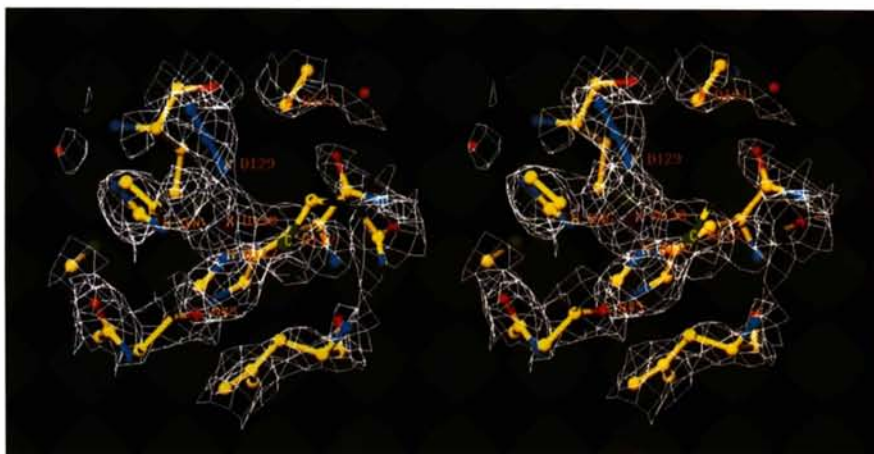


Fig. 3. The copper site in the Met121Ala-azide mutant,  $2F_o - F_c$  electron-density maps contoured at  $1.0\sigma$ .

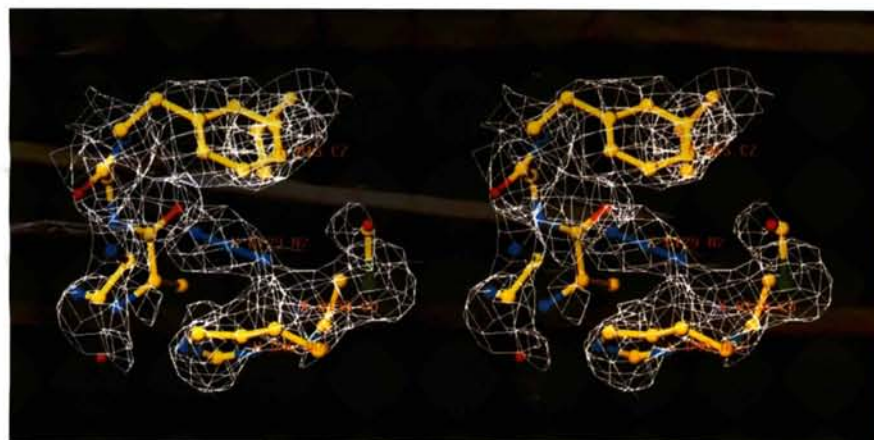


Fig. 4. The mutation site in the Met121Ala-azide mutant,  $2F_o - F_c$  electron-density maps contoured at  $1.0\sigma$ . The azide molecule exhibits  $\pi$  overlap with His46 and Phe15.

## 2. Materials and methods

### 2.1. DNA techniques, expression and purification

The DNA techniques have been described previously (Karlsson, Aasa, Malmström & Lundberg, 1989). The azurin mutant was expressed in *Escherichia coli* strain RV308 and fermented in a 1 l LB media shake culture (16 h).  $\text{CuCl}_2$  (100  $\mu\text{M}$ ), ampicillin (100  $\text{mg l}^{-1}$ ) and isopropyl- $\beta$ -D-thiogalactopyranoside (IPTG, 0.5  $\text{mM}$ ) were added when the cultivation was started. The purification of Met121Ala was carried out according to Karlsson, Pascher, Nordling, Arvidsson & Lundberg (1989), except that the sample was gel-filtrated using Sephadex S-100 gel in 100  $\text{mM}$  phosphate buffer. The sample was checked on a sodium dodecyl sulfate polyacrylamide gel electrophoresis (SDS-PAGE) denaturing gel with  $\beta$ -mercaptoethanol, showing that the sample only contained azurin. A final purification step was also included to remove the apo and Zn-coordinated protein. This was an anionic exchange chromatography step on a Waters Q8 HR column. The copper was reduced with 100  $\mu\text{M}$  ascorbic acid, and thereby the copper-containing azurin could be separated from apo and Zn azurin since  $\text{Cu}^+$  azurin has a  $pI$  of 4.6 ( $\text{Cu}^{2+}\text{Az}$ ,  $pI$  5.6;  $\text{Zn}^{2+}\text{Az}$ ,  $pI$  5.4; apoAz,  $pI$  5.8). Similarly, denatured azurin which has a  $pI$  of 6.2 (van de Kamp, Hali, Rosato, Finazzi-Agro & Canters, 1990) was also removed. The sample was applied in 20  $\text{mM}$  Tris-HCl pH 8.3 to which 100  $\mu\text{M}$   $\text{CuCl}_2$  had been added, and eluted with a gradient of 0–80  $\text{mM}$  NaCl. These experiments were performed at room temperature. The fractions containing the copper Met121Ala were pooled and concentrated using an ultrafiltration unit and dialyzed against deionized water for 48 h at 277 K before the crystallization experiment.

### 2.2. Gel analysis

The SDS-PAGE gel analysis was performed on a Pharmacia PhastSystem using Pharmacia SDS-PAGE gradient 8–25% gels under reducing conditions.

### 2.3. Spectroscopy

The UV-visible and EPR spectra were recorded on a Cary 4.0 spectrophotometer and a Bruker ER 200D-SRC spectrometer, respectively. The concentration of  $\text{Cu}^{2+}$  was obtained from integration of EPR spectra as described earlier (Aasa & Vänngård, 1975).

### 2.4. Reduction potential determination

The reduction potentials were measured with the optically transparent thin-layer electrolysis technique at 298 K, using Tris(1,10-phenanthroline)cobalt(III) perchlorate as the redox mediator (Pascher, Karlsson, Nordling, Malmström & Vänngård, 1993). A Methron (6.07001.100) saturated calomel electrode (SCE) was used as reference electrode. The mutant and the mediator had a concentration of 50  $\mu\text{M}$ . The concentration of azide

in the Met121Ala-azide sample was 20  $\text{mM}$  and the redox state was monitored at 410 nm. The reduction potential measurements were performed in 10  $\text{mM}$  Hepes, 100  $\text{mM}$  KCl pH 7.0 at 298 K versus normal hydrogen electrode.

### 2.5. Crystallization and data collection

Blue Met121Ala crystals were formed from a solution containing 3.2  $\text{M}$  ammonium sulfate and 0.5  $\text{M}$  lithium nitrate at pH 5.1 and a temperature of 297–298 K, in around 15 d. The largest crystal of this form was about  $0.4 \times 0.3 \times 0.2$  mm. The crystals were found to be orthorhombic, space group  $P2_12_12_1$ , with cell constants  $a = 109.4$ ,  $b = 98.8$ ,  $c = 48.0$  Å, and isomorphous to the nickel-substituted azurin crystal, with cell constants  $a = 110.2$ ,  $b = 99.5$ ,  $c = 48.3$  Å. The crystal structure contains four molecules/asymmetric unit.

X-ray diffraction data from the Met121Ala mutant crystal were collected on an Enraf-Nonius FAST television system diffractometer.  $\text{Cu K}\alpha$  radiation from a FR571 generator operating at 40 kW and 50 mA with the focal spot size of  $0.2 \times 2$  mm was used. The reflection data were evaluated on-line using the program MADNES (Messerschmidt & Pflugrath, 1987). Two data sets containing 14 626 (12–2.6 Å) and 24 018 (8–2.2 Å) reflections were collected from two crystals. After merging the two data sets, 24 707 reflections to a resolution of 2.2 Å were obtained.

Using the same diffractometer, a data set was collected from a Met121Ala crystal which was soaked in a solution composed of 3.2  $\text{M}$   $\text{NH}_4(\text{SO}_4)_2$ , 0.5  $\text{M}$   $\text{LiNO}_3$  and 0.1%  $\text{NaN}_3$  for 15 min before data collection. 18 193 unique reflections to 2.3 Å resolution were collected. The completeness of data into various resolution intervals has been summarized in Table 1.

### 2.6. Structure solution and refinement

Coordinates of the nickel-substituted azurin from *Pseudomonas aeruginosa* (Bonander *et al.*, 1996) were used as the starting set for the structure determination. Structure factors and electron-density maps for the Met121Ala mutant and its azide derivative were calculated from the nickel-substituted model phases with solvent molecules and the atoms of the mutation site omitted. Crystallographic refinement was carried out with energy restraints using the X-PLOR program (Brünger, 1992). The copper sites were refined without energy restraints. After a conjugate-gradient energy-restrained positional refinement followed by a restrained  $B$ -factor refinement ( $R = 28\%$ ), electron-density maps were calculated. The maps ( $2F_o - F_c$ ) were inspected and the coordinates were manually corrected on a graphics display (Evans & Sutherland) using the program FRODO (Jones, 1978). Particularly the coordinates from the water structure, initially adopted from the model, were inspected and waters were added or

Table 1. Summary of data reduction

Resolution range (Å)	Observed No. of unique reflections	Expected No. of unique reflections	$R_{\text{merge}}$	Completeness (%)
<i>(a) Data set 1 of Met121Ala</i>				
12.280–5.717	1359	1533	3.9	88.7
5.717–4.531	1530	1642	3.7	93.2
4.531–3.933	1591	1702	4.2	93.5
3.933–3.550	1661	1754	4.2	94.7
3.550–3.277	1678	1787	4.4	93.9
2.277–3.069	1692	1812	5.1	93.4
3.069–2.902	1695	1848	6.4	91.7
2.902–2.765	1679	1861	6.9	90.2
2.765–2.648	1351	1904	7.3	70.9
2.648–2.549	390	1891	8.3	20.6
<i>(b) Data set 2 of Met121Ala</i>				
8.175–4.667	2300	2471	3.7	93.1
4.667–3.770	2518	2638	4.3	95.4
3.770–3.295	2647	2743	6.0	96.5
3.295–2.986	2712	2815	8.2	96.3
2.986–2.762	2800	2886	11.4	97.0
2.762–2.591	2785	2913	13.5	95.6
2.591–2.453	2752	2971	16.3	92.6
2.453–2.339	2729	3003	18.6	90.9
2.339–2.242	2294	3052	20.5	75.2
2.242–2.159	481	3060	16.2	15.7
<i>(c) Data set of Met121Ala-azide</i>				
10.785–5.127	1809	2079	7.1	87.0
5.127–4.069	2014	2235	6.8	90.1
4.069–3.534	2138	2319	7.3	92.2
3.534–3.191	2188	2390	7.9	91.6
3.191–2.946	2152	2439	9.9	88.2
2.946–2.759	2096	2478	12.0	84.6
2.759–2.609	2026	2525	14.1	80.2
2.609–2.486	1961	2543	16.1	77.1
2.486–2.382	1481	2574	18.8	57.5
2.382–2.292	328	2615	18.6	12.5

deleted according to indications in the Fourier map and, in addition, the formation of reasonable hydrogen bonds. During the subsequent conjugate-gradient energy-restrained positional and  $B$ -factor refinements the  $R$  value dropped to 21.3% for Met121Ala mutant and 19.4% for Met121Ala-azide. The details of the refinement of these two mutant structures are listed in Table 2.  $R$ -free parameters were not monitored during the refinement. Non-crystallographic symmetry refinement was not utilized. A comparison of the four molecules in the asymmetric unit and with the wild-type protein (Nar, Messerschmidt, Huber, van de Kamp & Canters, 1991), is given in Table 3.

### 3. Results

#### 3.1. The structure

The final model for Met121Ala mutant consists of 3888 protein atoms and 231 water molecules, and the final model for Met121Ala-azide derivative consists of 3888 protein atoms and 224 water molecules and, in addition, one azide anion in each of the four molecules in the asymmetric unit. The final crystallographic  $R$  value

Table 2. Data-collection parameters

	Met121Ala (1+2)	Met121Ala-azide
Crystal size (mm)	$0.4 \times 0.3 \times 0.2$	$0.4 \times 0.3 \times 0.2$
Space group	$P2_12_12_1$	$P2_12_12_1$
Unit-cell constants (Å)		
$a$	109.4	109.7
$b$	98.8	98.7
$c$	48.0	48.1
Total No. of measurements	100294	36479
Total No. of unique reflections	24707	18193
Data completeness (%)	93	84
Reflection averaging $R_m^*$ (%)	4.7	7.9
No. of atoms used in refinement	4119	4124
Protein atoms	3888	3888
Solvent	231	224
Azide anions	—	12
Resolution range used in the refinement (Å)	8–2.2	8–2.3
Root-mean-square deviation		
Bonds (Å)	0.023	0.023
Angles (°)	2.41	2.46
$R$ value (%)†	21.3	19.4

\*  $R_m = \sum_H \sum_{i=1}^N |I(H)_i - \langle I(H) \rangle| / \sum_H \sum_{i=1}^N I(H)_i$ , where  $I(H)_i$  is the  $i$ th measurement of reflection  $H$ ,  $\langle I(H) \rangle$  is its mean value and the summation extends over all the reflections more than once in the set. †  $R = \sum |F_o - F_c| / \sum |F_o|$ .

Table 3.  $R.m.s.$  deviations calculated from a superposition of the native azurin and the four monomers A–D

The four  $r.m.s.$  values per block (Å) indicated values for  $C^\alpha$  atoms, main-chain atoms, side-chain atoms and all atoms.

#### (a) Met121Ala azurin mutant

	Azurin-A	Azurin-B	Azurin-C	Azurin-D
$C^\alpha$ atoms	0.492	0.403	0.477	0.408
Main-chain atoms	0.529	0.462	0.494	0.464
Side-chain atoms	1.235	1.438	1.280	1.185
All atoms	0.930	1.041	0.948	0.879

#### (b) Met121Ala-azide mutant

	Azurin-A	Azurin-B	Azurin-C	Azurin-D
$C^\alpha$ atoms	0.481	0.434	0.453	0.425
Main-chain atoms	0.523	0.490	0.501	0.490
Side-chain atoms	1.247	1.457	1.292	1.204
All atoms	0.935	1.060	0.957	0.898

#### (c) Superposition of each of the four monomers in Met121Ala-azide mutant

	A-B	A-C	A-D	B-C	B-D	C-D
$C^\alpha$ atoms	0.409	0.402	0.430	0.300	0.484	0.477
Main-chain atoms	0.438	0.458	0.486	0.338	0.512	0.509
Side-chain atoms	1.436	1.224	1.268	1.086	1.436	1.161
All atoms	1.037	0.905	0.940	0.786	1.055	0.879

for Met121Ala is 21.3% for 24 707 reflections to 2.2 Å resolution and for Met121Ala-azide derivative 19.4% for 18193 reflections to 2.3 Å resolution. Most of the structures are well defined, especially the  $\beta$ -strands, the loops around the copper site and all internal side chains. They have relatively low  $B$  factors, 5–20 Å<sup>2</sup>. The N- and C-terminal chains and the residues at position 2 have

Table 4. Copper-site geometry in both Met121Ala and Met121Ala-azide mutant structures as compared to wild-type azurin and ascorbate oxidase azide form

(a) Cu-ligand bond lengths (Å)				
	Met121Ala	Met121Ala-azide	Ascorbate oxidase azide form	Azurin (pH 5.5)
Cu—O(45)	2.74 (7)	3.18 (7)		2.97
Cu—N <sup>δ1</sup> (46)	2.21 (3)	2.23 (9)		2.11
Cu—S <sup>γ</sup> (112)	2.12 (7)	2.32 (6)	N <sup>2</sup> (106) 2.11	2.25
Cu—N <sup>δ1</sup> (117)	2.37 (2)	2.37 (6)	N <sup>2</sup> (450) 2.11	2.03
Cu-trigonal planes	0.04 (5)	0.26 (8)	N <sup>2</sup> (506) 2.11	
Cu—N1 (azide 2)		2.04 (4)	1.99	
N1—N2 (azide 1)		1.17 (2)	1.15	
N2—N3 (azide 1)		1.16 (1)	1.15	
Cu—N1 (azide 2)			1.97	
N1—N2 (azide 2)			1.18	
N2—N3 (azide 2)			1.18	
Cu—C <sup>β</sup> (121)	4.75 (8)	4.62 (8)		5.01
Cu—S <sup>δ</sup> (121)				3.15
C <sup>α</sup> (45)—C <sup>α</sup> (121)	11.24 (8)	11.42 (9)		11.65
O(45)—C <sup>α</sup> (121)	9.02 (8)	9.26 (10)		9.42
(b) Bond angles around the copper (°)				
	Met121Ala	Met121Ala -azide	Ascorbate oxidase azide form	Azurin (pH 5.5)
(45) O—Cu—N <sup>δ1</sup> (46)	80 (7)	76 (4)		73
(45) O—Cu—S <sup>γ</sup> (112)	98 (3)	92 (8)		98
(45) O—Cu—N <sup>δ1</sup> (117)	86 (2)	81 (3)		89
(45) O—Cu—N1 (azide), S <sup>δ</sup> (121)		147 (8)		149
(46) N <sup>δ1</sup> —Cu—S <sup>γ</sup> (112)	135 (3)	138 (8)		133
(46) N <sup>δ1</sup> —Cu—N <sup>δ1</sup> (117)	98 (6)	102 (8)		103
(46) N <sup>δ1</sup> —Cu—N1 (azide), S <sup>δ</sup> (121)		74 (6)		78
(112) S <sup>γ</sup> —Cu—N <sup>δ1</sup> (117)	127 (5)	115 (8)		123
(112) S <sup>γ</sup> —Cu—N1 (azide), S <sup>δ</sup> (121)		103 (5)		110
(117) N <sup>δ1</sup> —Cu—N1 (azide), S <sup>δ</sup> (121)		115 (14)		87
(azide1) N2—N1—Cu		136 (4)	125	
(azide1) N3—N2—N1		177 (1)	128	
(azide2) N2—N1—Cu			109	
(azide2) N3—N2—N1			173	
(121) C <sup>γ</sup> —S <sup>δ</sup> —Cu				140

higher *B* factors, 50–70 Å<sup>2</sup>. The Ramachandran plots (Ramachandran, Ramakrishnan & Sasisekharan, 1963; Ramachandran & Sasisekharan, 1968) of the dihedral angles are given in Figs. 1(a) and 1(b). The 2*F*<sub>o</sub>−*F*<sub>c</sub> maps contoured at 1σ level show continuous density for all main-chain atoms. The four molecules in the asymmetric unit are packed as a dimer of dimers. The packing of the dimer in this mutant is very similar to the dimer packing in the wild-type structure.

In Fig. 2(a), 2*F*<sub>o</sub>−*F*<sub>c</sub> electron-density maps covering the copper site in the Met121Ala mutant structure are shown. These maps have been calculated using phases from the nickel-substituted azurin with solvent molecules and the atoms at the mutation site omitted. As it can be seen, there is a pocket between the copper ion and the C<sup>β</sup> of Ala121. No extra density was found in this pocket. In addition, the copper ion has moved slightly towards the carbonyl O atom of Gly45, the distance between the copper and O=C of Gly45 being about 2.74 Å. The copper is thereby coordinated by

four ligands (Gly45, His46, Cys112 and His117) and its geometry can be described as a highly distorted tetrahedron, although the interaction with the Gly45 O atom is weak.

For the Met121Ala-azide derivative, the electron-density maps were also obtained using phases from the nickel-substituted azurin. The 2*F*<sub>o</sub>−*F*<sub>c</sub> maps of the Met121Ala-azide derivative show a significant density peak in the neighborhood of the copper ion (Fig. 2b). It was readily modeled as an azide anion which was included in the next set of refinement cycles. The distance between the end N atom of the azide anion to the copper ion is 2.04 Å. Thus, the copper has four ligands (His46, Cys112, His117 and the azide anion) and its geometry can be described as a distorted tetrahedron with the fourth ligand azide anion in the apical position (Fig. 3). In addition, the azide anion exhibits a π electron overlap with the ring system of residue Phe15 and His46 (Fig. 4). The copper-site geometries of the wild-type azurin and the Met121Ala mutant and its azide derivative are

summarized in Table 4. In addition, the azide copper-site geometry of the ascorbate oxidase is included for comparison.

### 3.2. Spectroscopic characterization

The EPR spectra of a frozen solution of the wild-type azurin protein, the mutant Met121Ala and the Met121Ala-azide derivative are presented in Fig. 5. While the two spectra from the wild-type azurin and the Met121Ala mutant are rather similar and show the typical unique hyperfine splitting, the EPR spectrum from Met121Ala-azide derivative is quite different. The hyperfine splitting is much larger and the spectrum is thus considered to be a modified type I site. The visible region of the spectrum is presented as a function of the increasing amount of azide added to the Met121Ala mutant in Fig. 6. It is clearly seen that the two optical absorption bands in the Ala121 mutant at 629 and 460 nm are shifted towards higher energy, 520 and 410 nm, respectively. Concomitantly, the low-energy absorption decreases and the high-energy absorption increases. The equilibrium dissociation constant at 293 K was determined to be 6 mM. The EPR and optical absorption parameters are summarized in Table 5.

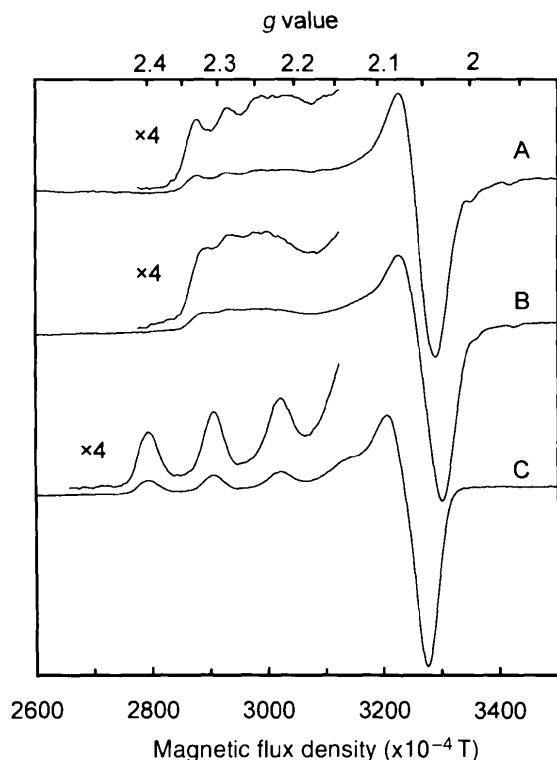


Fig. 5. X-band EPR spectra showing wild-type azurin (A), Met121Ala (B) and Met121Ala + 10 mM  $N_3^-$  (C). Spectrometer conditions: microwave frequency, 9.38 GHz; microwave power, 2 mW; modulation amplitude, 2 mT; temperature 77 K. The low-field part of the spectra is also shown at four times higher gain.

Table 5. Main optical band maximum and EPR properties of wild-type azurin and azurin mutant Met121Ala and Met121Ala-azide and their reduction potentials

$g_{\parallel}$  and  $g_{\perp}$  are g values in the parallel and perpendicular direction, respectively, and  $A_{\parallel}$  is the hyperfine coupling in the parallel direction.

#### (a) EPR properties

Protein	EPR parameters			$\lambda_{\max}$ (nm)
	$g_{\parallel}$	$A_{\parallel}$ (G)	$g_{\perp}$	
Wild type	2.261	53	2.059	628
Met121Ala	2.258	50	2.04	629
Met121Ala-azide	2.263	112	2.06	409

#### (b) Reduction potentials at pH 7

Protein	$E^0$ (mV)
Wild type	310*
Met121Ala	373*
Met121Ala-azide	330

\* From Pascher, Karlsson, Nordling, Malmström & Vänngård (1993).

## 4. Discussion

### 4.1. The Met121Ala mutant

The coordination in the copper site in wild-type azurin is known to be stable and protecting the copper ion. This is, for instance, demonstrated by the fact that the protein is denatured only at temperatures above 348 K and the EPR spectrum of the wild-type protein does not show any change upon additions of rather high concentrations (10 mM) of small inorganic liganding anions such as cyanide or azide.

When, however, the Met121 amino-acid residue is exchanged for the very much smaller alanine residue, a 'pocket' occurs between the  $C\beta$  of this residue and the copper ion. This pocket is, in principle, large enough to accommodate small organic or inorganic molecules. If a water molecule became trapped in this pocket, it would probably have induced a change to a 'stellacyanin-like' EPR spectrum, but as can be seen from Fig. 5 this is not the case. An X-ray structure analysis was, therefore, motivated in order to examine if the geometry of the copper site might have changed such that neighboring side chains might have occupied parts of the pocket.

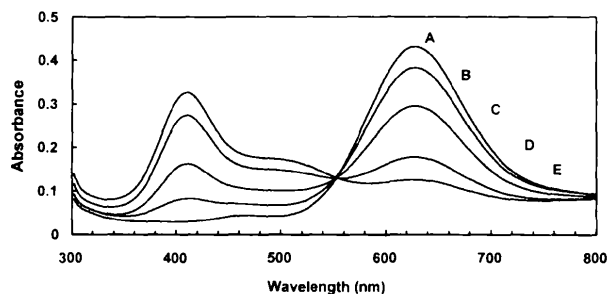


Fig. 6. Optical absorbance of the Met121Ala mutant with increasing amount of azide. No addition (A); 0.6 mM (B); 2.5 mM (C); 10 mM (D); 21 mM  $N_3^-$  (E).

However, the Fourier electron-density maps based on the refined Met121Ala azurin mutant structure do not show any additional density in this region of the molecule and the coordinates obtained from the least-squares refinement also indicate that the movement of the ligands to the copper ion, or the other side chains in the metal-site compartment, is very small. In addition, in Hubbard, Gross & Argos (1994), it is demonstrated that cavities that do not contain water are present in a number of proteins, in particular when the amino acids lining the cavity walls are Leu, Ile and Phe. The cavity in azurin is indeed surrounded by hydrophobic amino acids. The conclusion is therefore that the free space in the apical direction from the trigonal plane in the copper site in this mutant is large enough to accommodate small molecules.

The Met121Ala mutant crystal structure is on the whole very similar to the wild-type protein (Nar *et al.*, 1991) and shows the same stability pattern. As usual, the  $\beta$  structure in the protein has lower temperature factors than the connecting turns and the N and C termini. However, there are some small differences in the copper-site geometry compared with the wild-type protein. The distances stated in Table 4 represent the mean distances based on four independent mutant molecules in the asymmetric unit. The significant differences in bond lengths in the copper site between the Met121Ala mutant and the wild-type structure, are the Cu—N $\delta$  (His117) and O (Gly45)—C $\alpha$  (residue 121) distances. The His117 imidazole side chain seems to have moved away slightly from the copper ion since the copper ion evidently remains in the trigonal plane (Table 4, Fig. 7). The distance between the apical O atom of Gly45 and the Ca of Ala121 in the mutant is 9.02 Å compared with 9.42 Å in the wild-type structure suggesting that the copper site has overall become compressed along the apical direction. Even if the distance from the copper ion to the apical O atom of Gly45 has decreased by 0.23 Å, the difference is to be considered significant based in the accuracy of the solution (argued from a  $3\sigma$  level).

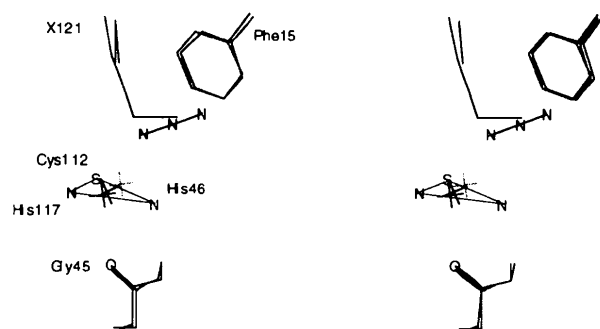


Fig. 7. Stereoview of the superimposed copper site of wild-type azurin, Met121Ala and Met121Ala-azide. The Cu atom is symbolized as a cross (grey cross, Met121Ala-azide; black cross, wild type and Met121Ala). The amino-acid X121, is either Ala or Met (wild type). The trigonal plane is indicated the amino acids His46, Cys112 and His117 in wild-type azurin.

The spectroscopic data in Table 4 also confirm that structural changes introduced by the mutation Met121Ala are minor. The EPR and optical spectra of the Met121Ala are very similar to that of the wild-type azurin. The reduction potential, on the other hand, has increased considerably (by 63 mV, see Table 5). This is a consequence of the replacement of the methionine with a hydrophobic alanine. It also supports the conclusion above that a water molecule is not embedded in the cavity. A polarizable water molecule close to the copper ion would lower the potential, as in the mutant where a stop codon was introduced in position 121 (Pascher *et al.*, 1993). This leads to an open structure allowing water entry which results in a reduction potential reduced by over one third (from 310 to 205 mV).

#### 4.2. The azide derivative of the Met121Ala mutant

In the Met121Ala-azide azurin structure, the copper site is now described as a distorted tetrahedral geometry with four strong bonds formed between the copper ion and the three ligands from the amino-acid residues His46, Cys112 and His117, and, in addition, the azide anion. The copper ion has moved about 0.26 Å out of the trigonal plane formed by the three liganding amino-acid residues, and forms a strong bond with the azide anion (Table 4, Fig. 7). The azide anion has subsequently occupied a part of the free space in the apical direction around the Ala121 amino-acid residue and the copper–nitrogen distance is refined to be 2.04 Å (Figs. 2*b* and 3).

When azide is added to the Met121Ala mutant solution the measured EPR spectra indicate that the copper site changes from a type I site to a modified type I site. The binding of azide can also be followed by measuring the optical absorption spectrum. In Fig. 6 it is shown that the binding of azide produces a broad absorption in the 350 to 500 nm region and a rather well defined maximum at 409 nm. This is another indication of an altered copper site from type I into a modified type I. Since the cysteine S atom is still bound to the copper, this band is at least in part due to a S—Cu charge-transfer band similar to that found in the Met121Glu mutant. Contributions from an azide–Cu charge-transfer band cannot be excluded, since such bands appear in this region with considerable intensity ( $10^3 M^{-1}cm^{-1}$ ). However, a similar spectrum is observed for the Lys121 mutant at pH 7 demonstrating that optical bands in this region do not require charged ligands (Karlsson *et al.*, 1991).

The dissociation constant for the azide binding (6 mM) is about two times smaller than that of the azide binding to superoxide dismutase (Mota de Freitas & Valentine, 1984). This is in line with the stabilizing effect of the residues surrounding azide in the Met121Ala mutant. Azide binding also lowers the reduction potential by about 40 mV. In part, this may result from the introduction of an electron-donating azide anion, which stabilizes the divalent state of the copper.



It is interesting to compare the copper site in the Met121Ala-azide derivative with the similar azide-modified copper site in ascorbate oxidase (Messerschmidt *et al.*, 1993). In wild-type ascorbate oxidase the copper ion marked Cu2 is one of the type 3 pairs (Cu2—Cu3) and it is coordinated to three histidine N atoms in a trigonal arrangement. This site is accessible to the bulk water and consequently azide anions or other small molecules may have access to the site. It was found that two azide molecules bind directly to the copper ion in the Cu2 site and the ligands form a distorted trigonal bipyramid where the azide anions occupy the apical directions. The bond distances in azide derivative of ascorbate oxidase copper site are presented in Table 4. The distances between the copper and the azide N atom are similar in the two structures within the accuracy of the determination.

#### 4.3. Concluding remarks

The conclusion from the X-ray structure solution of the two structures, Met121Ala and Met121Ala-azide, is that the cavity which occurs in the Met121Ala mutant is not occupied by a water molecule, supporting the finding that the optical and EPR data are similar to the wild-type azurin. The methionine in position 121 in addition to modulating the properties of the copper ion also makes the copper site inaccessible to exogenous ligands. The copper site is therefore less sensitive to changes in the environment which otherwise would alter the physical properties of the copper site upon exposure to small ligands. A mutation of the methionine to the small hydrophobic alanine residue opens up the possibility to further tune the properties of this protein by adding an exogenous ligand. This in turn can be used as a complement to the normal procedure in tuning the properties which involves a site-specific mutation to other amino-acid residues in position 121 or in the close neighborhood of the copper site.\*

We would like to thank the Swedish Natural Science Research Council and the Bio-Väst Foundation for Biotechnology for financial support of this project.

\* Atomic coordinates and structure factors have been deposited with the Protein Data Bank, Brookhaven National Laboratory (Reference: 2TSA, R2TSASF; 2TSB, R2TSBSF). Free copies may be obtained through The Managing Editor, International Union of Crystallography, 5 Abbey Square, Chester CH1 2HU, England (Reference: HE0140).

#### References

- Aasa, R. & Vänngård, T. (1975). *J. Magn. Res.* **19**, 308–315.  
 Adman, E. T. (1991). *Adv. Protein Chem.* **42**, 145–197.  
 Adman, E. T., Stenkamp, R. E., Sieker, L. C. & Jensen, L. H. (1978). *J. Mol. Biol.* **123**, 35–45.  
 den Blaauwen, T. & Canters, G. W. (1993). *J. Am. Chem. Soc.* **115**, 1121–1129.  
 den Blaauwen, T., van de Kamp, M. & Canters, G. W. (1991). *J. Am. Chem. Soc.* **113**, 5050–5052.  
 Bonander, N., Karlsson, B. G. & Vänngård, T. (1996). *Biochemistry*. In the press.  
 Bonander, N., Vänngård, T., Tsai, L.-C., Langer, V., Nar, H. & Sjölin, L. (1996). *J. Biol. Inorg. Chem.* Submitted.  
 Brünger, A. T. (1992). *X-PLOR Version 3.1, Manual*. Yale University, New Haven, CT, USA.  
 Chang, T. K., Iverson, S. A., Rodrigues, C. G., Kiser, C. N., Lew, A. Y. C., Germanas, J. P. & Richards, J. H. (1991). *Proc. Natl Acad. Sci. USA*, **88**, 1325–1329.  
 Colman, P. M., Freeman, H. C., Guss, J. M., Murata, M., Norris, V. A., Ramshaw, J. A. M. & Venkatappa, M. P. (1978). *Nature (London)*, **272**, 319–324.  
 Dodd, F. E., Hasnain, S. S., Abraham, Z. H. L., Eady, R. R. & Smith, B. E. (1995). *Acta Cryst. D51*, 1052–1064.  
 Fields, B. A., Guss, J. M. & Freeman, H. C. (1991). *J. Mol. Biol.* **222**, 1053–1065.  
 Gray, H. B. & Malmström, B. G. (1983). *Comments Inorg. Chem.* **2**, 203–209.  
 Hubbard, S. J., Gross, K.-H. & Argos, P. (1994). *Protein Eng.* **7**, 613–626.  
 Jones, T. A. (1978). *J. Appl. Cryst.* **11**, 268–272.  
 van de Kamp, M., Hali, F. C., Rosato, N., Finazzi-Agro, A. & Canters, G. W. (1990). *Biochim. Biophys. Acta*, **1019**, 283–292.  
 Karlsson, B. G., Aasa, R., Malmström, B. G. & Lundberg, L. G. (1989). *FEBS Lett.* **253**, 99–102.  
 Karlsson, B. G., Nordling, M., Pascher, T., Tsai, L. C., Sjölin, L. & Lundberg, L. G. (1991). *Protein Eng.* **4**, 343–349.  
 Karlsson, B. G., Pascher, T., Nordling, M., Arvidsson, R. H. A. & Lundberg, L. G. (1989). *FEBS Lett.* **246**, 211–217.  
 Karlsson, B. G., Tsai, L.-C., Nar, H., Sanders-Loehr, J., Bonander, N., Langer, V. & Sjölin, L. (1996). *Biochemistry*. Submitted.  
 Laskowski, R. A., MacArthur, M. W., Moss, D. S. & Thornton, J. M. (1993). *J. Appl. Cryst.* **26**, 283–291.  
 Mota de Freitas, D. & Valentine, J. S. (1984). *Biochemistry*, **23**, 2079–2082.  
 Messerschmidt, A., Luecke, H. & Huber, R. (1993). *J. Mol. Biol.* **230**, 997–1014.  
 Messerschmidt, A. & Pflugrath, J. W. (1987). *J. Appl. Cryst.* **20**, 306–315.  
 Mizoguchi, T. J., di Bilio, A. J., Gray, H. B. & Richards, J. H. (1992). *J. Am. Chem. Soc.* **114**, 10076–10078.  
 Nar, H., Messerschmidt, A., Huber, R., van de Kamp, M. & Canters, G. W. (1991). *J. Mol. Biol.* **221**, 765–776.  
 Pascher, T., Karlsson, B. G., Nordling, M., Malmström, B. G. & Vänngård, T. (1993). *Eur. J. Biochem.* **212**, 289–296.  
 Ramachandran, G. N., Ramakrishnan, C. & Sasisekharan, V. (1963). *J. Mol. Biol.* **7**, 995.  
 Ramachandran, G. N. & Sasisekharan, V. (1968). *Adv. Protein Chem.* **23**, 238.  
 Reinhammar, B. (1972). *Biochim. Biophys. Acta*, **275**, 245–259.  
 Romero, A., Hoitink, C. W. G., Nar, H., Huber, R., Messerschmidt, A. & Canters, G. W. (1993). *J. Mol. Biol.* **229**, 1007–1021.